Regulation of Microtubule Dynamic Instability by Tubulin-GDP†

André Vandecandelaere,* Stephen R. Martin, and Peter M. Bayley

Division of Physical Biochemistry, National Institute for Medical Research, Mill Hill, London NW7 1AA, U.K.

Received July 12, 1994; Revised Manuscript Received October 19, 1994⊗

ABSTRACT: The regulation of the spontaneous transitions between growth and shortening of microtubules is central to the biological function of dynamic instability. Here we examine the effects of controlled amounts of tubulin-GDP (Tu-GDP) on the dynamic properties of microtubules *in vitro*. The transphosphorylation equilibrium between GTP, GDP, UTP, and UDP in the presence of nucleoside-5′-diphosphate kinase (NDPK) was used to fix the ratio x_D = [Tu-GDP]/([Tu-GTP] + [Tu-GDP]) in solution. Lower levels of Tu-GDP (x_D < 0.6) produce only a small increase in the apparent critical concentration, C_c'. However, at x_D > 0.6 a dramatic increase in C_c is observed. At steady state of assembly, low levels of Tu-GDP (x_D < 0.5) cause a significant reduction of the dynamic length redistribution of the microtubule population. The principal observable effect of Tu-GDP on the empirical parameters of microtubule dynamic instability is to decrease the duration of individual phases of microtubule growth and shortening, with relatively little effect on the intrinsic rates of growth and shortening. Observations in dark-field video microscopy reveal that the irregularities in the rates of growth (and shortening) are increased in the presence of Tu-GDP. At elevated levels of Tu-GDP, pauses occur frequently during the growth phase, microtubule dynamics cease to conform to a clear two-phase process, and the extents of growth and shortening excursions are strongly attenuated. The experimental results are well reproduced by computer simulation, using mechanisms defined in the lateral cap model for dynamic instability [Martin, S. R., Schilstra, M. J., & Bayley, P. M. (1993) *Biophys. J. 65,* 578−596], which includes the binding of Tu-GDP to the microtubule end in competition with Tu-GTP. In the presence of Tu-GDP, the growing-state lifetime is significantly attenuated, and the microtubule length versus time excursions simulated by the model show irregularities and complex multistate behavior, including pauses, as observed experimentally. These results suggest that Tu-GDP can modulate microtubule dynamics significantly under conditions where little bulk microtubule disassembly is induced. Tu-GDP therefore appears to exemplify the action of a relatively simple factor with the potential capability for regulation of microtubule dynamics in a cellular environment.

Microtubules are polymeric protein assemblies consisting of essentially linear protofilaments of the 100-kDa tubulin $\alpha\beta$-heterodimer arranged parallel to a cylindrical axis. The surface lattice shows a helical arrangement for the individual tubulin molecules (Amos, 1979). The diameter of microtubules varies only within small limits (depending on the number of protofilaments, which ranges from 12 to 17), and they may be several tens of micrometers in length (1625 tubulin dimers per micrometer for a 13-protofilament structure). They are present in abundance in eukaryotic cells, and they are involved in a variety of functions such as intracellular transport, structure and shape determination, and cell motility and division (Dustin, 1978; Roberts & Hyams, 1979; Hyams & Lloyd, 1994).

The tubulin dimer is isolated by repeated cycles of assembly and disassembly and contains two binding sites for guanine nucleotides, only one of which (the E-site, β-subunit) contains exchangeably bound nucleotide (Weisenberg et al., 1968; Berry & Shelanski, 1972). The affinity of GTP for the tubulin E-site depends upon the Mg^{2+} concentration (Zeeberg & Caplow, 1979; Correia et al., 1987; Mejillano & Himes, 1991). In contrast, the affinity of the tubulin E-site for GDP is independent of [Mg^{2+}] (K_d = 0.2 μM in PIPES[1] buffer at 4 °C; Mejillano & Himes, 1991). In the absence of Mg^{2+} the affinity for GTP is more than 10 times lower than that for GDP. In the presence of Mg^{2+}, however, the affinity for GTP is more than 2 times greater than that for GDP: values for the ratio of association constants, K_{GTP}/K_{GDP}, between 2.1 and 6 have been reported [2.8 at 22 °C (Zeeberg & Caplow, 1979); 4.86 at 21 °C (Fishback & Yarbrough, 1984); 6 at 37 °C (Carlier & Pantaloni, 1978); 2.1 at 37 °C (Kristofferson et al., 1982);

† This work was supported *in part* by EC Twinning Grant 902/00203.

* Mailing address: Division of Physical Biochemistry, National Institute for Medical Research, The Ridgeway, Mill Hill, London NW7 1AA, U.K. Phone: 081-959-3666, ext. 2085. Fax: 081-906-4477.

⊗ Abstract published in *Advance ACS Abstracts,* January 1, 1995.

[1] Abbreviations: Tu-GTP, the tubulin $\alpha\beta$-heterodimer with GTP at the exchangeable nucleotide binding site (E-site); Tu-GDP, the tubulin $\alpha\beta$-heterodimer with GDP at the E-site; MAPs, microtubule associated proteins; Mes, 2-(*N*-morpholino)ethanesulfonic acid; PEM, microtubule assembly buffer containing 100 mM 1,4-piperazinediethanesulfonic acid (Pipes), 0.1 mM ethylene glycol bis(β-aminoethyl ether)-*N,N,N′,N′*-tetraacetic acid (EGTA), and 1.7 mM $MgCl_2$ at pH 6.5; PEMG, PEM buffer containing 1 M glycerol; EGS, ethylene glycol bis(succinic acid *N*-hydroxysuccinimide ester); AK, acetate kinase; NDPK, nucleoside-5′-diphosphate kinase; x_D, mole fraction of Tu-GDP in the soluble phase (=[Tu-GDP]$_{sol}$/([Tu-GTP]$_{sol}$ + [Tu-GDP]$_{sol}$); k_{on}, k_{off}, empirical rate constants for dimer addition during growth and dimer loss during shortening, respectively, of a microtubule end; $k_{+,XY}$, $k_{-,XY}$, rate constants for addition and dissociation of a dimer at a site in the lattice, designated XY, where X and Y indicate the nucleotide (GTP or GDP) at the two neighboring sites; C_c, the critical concentration; C_c', the free dimer concentration, or the "apparent" critical concentration; C_s, the concentration of tubulin $\alpha\beta$-heterodimer in the soluble phase (=[Tu-GDP]$_{sol}$ + [Tu-GTP]$_{sol}$); C_t, the total concentration of tubulin in the system.

0006-2960/95/0434-1332$09.00/0

1.9−2.5 at 37 °C (Martin & Bayley, 1987); 2.1 at 4 °C (Mejillano & Himes, 1991)].

During microtubule assembly the E-site GTP is hydrolyzed to GDP and phosphate is released (Jacobs et al., 1974; Weisenberg et al., 1976). The hydrolysis of the nucleotide is not necessary for microtubule formation, since nonhydrolyzable analogues of GTP also support the assembly process (Weisenberg et al., 1976; Karr et al., 1979; Seckler et al., 1990; Mejillano et al., 1990). However, microtubules assembled from tubulin-GTP (Tu-GTP) display a remarkable steady-state behavior known as dynamic instability (Mitchison & Kirshner, 1984a,b; Horio & Hotani, 1986). In a population of microtubules at steady state of assembly, an individual microtubule interconverts, apparently at random, between periods of slow growth and relatively rapid shortening. A population of tubulin microtubules therefore consists of two subpopulations: slowly growing (G-state) microtubules (the majority) and rapidly shortening (S-state) microtubules. Under special conditions the transitions of the microtubules may be highly synchronized to produce oscillatory behavior (Carlier et al., 1987a; Mandelkow et al., 1988). Dynamic instability is suppressed when microtubule associated proteins (MAPs) or other stabilizing agents, such as taxol or glycerol, are present (Farrell et al., 1987; Hotani & Horio, 1988; Schilstra et al., 1991; Pryer et al., 1992; Drechsel et al., 1992; Kowalski & Williams, 1993a).

Dynamic instability behavior derives from the particular geometrical properties of the microtubule lattice and from the kinetic differences between Tu-GTP and Tu-GDP. Kinetic evidence suggests that the microtubule lattice consists of an unstable Tu-GDP core protected by a stabilizing structure originally termed the "Tu-GTP cap" (Pantaloni & Carlier, 1986). On this model a growing microtubule continues to grow so long as the rate of addition of Tu-GTP molecules is sufficiently high to maintain the cap. Loss of the cap exposes the unstable Tu-GDP core, and the microtubule enters the rapidly shortening state.

The nature and extent of any capping structure remain controversial since current experimental techniques do not permit the unequivocal resolution of the temporal relationship between dimer addition and GTP hydrolysis. If the hydrolysis of GTP is uncoupled from addition reactions, the size of the Tu-GTP cap can be large under the appropriate assembly conditions (Carlier & Pantaloni, 1981; Pantaloni & Carlier, 1986). However, other investigators failed to detect a significant Tu-GTP cap in microtubules at steady state, supporting the idea of tight coupling between GTP hydrolysis and the addition reaction (Schilstra et al., 1987; O'Brien et al., 1987, 1990; Stewart et al., 1990; Walker et al., 1991). In the limit, the stabilizing cap may be confined to a single terminal layer of Tu-GTP at the microtubule ends. Effective computer models for microtubule dynamic instability have been developed using the concept of a capping structure as a working hypothesis. The initial modeling employed random, uncoupled GTP hydrolysis (Chen & Hill, 1985). In the alternative case with tight coupling between dimer addition and GTP hydrolysis, Tu-GTP is confined to the terminal positions in the microtubule lattice, consistent with the above observations. This lateral cap model has been elaborated in detail using Monte Carlo computer simulation techniques (Martin et al.,1993; Bayley et al., 1990, 1994).

GDP inhibits both the extent and the rate of microtubule self-assembly and induces at least partial disassembly of preformed microtubules (Carlier & Pantaloni, 1978; Zackroff et al., 1980; Jameson & Caplow, 1980; Kristofferson et al., 1982). The addition of GDP to microtubule protein has an inhibitory effect on microtubule nucleation (Bayley et al., 1986). The amount of polymer existing in the presence of GDP depends on the relative nucleotide concentration ([GDP]/[GTP]) (Jameson & Caplow, 1980; Engelborghs & Van Houtte, 1981). The critical concentration for assembly of Tu-GDP is apparently very high, effectively infinite for practical purposes (Jameson & Caplow, 1980; Engelborghs & Van Houtte, 1981). The early observations on the effects of GDP were difficult to reconcile with the classical model for microtubule assembly (Oosawa & Asakura, 1975). In particular, the significant effects of GDP on microtubule self-assembly are difficult to reconcile with the limited GDP-induced disassembly of preformed microtubules and the small changes in the critical concentration, C_c. These observations led to doubts about the validity of the classical relation for condensation polymers, $C_c = k_{off}/k_{on}$ (with k_{on} and k_{off} being the empirical on and off rate constants for the equilibrium between polymers and free subunits), for microtubules in the presence of GDP (Zackroff et al., 1980).

These results present a rather confusing picture of the effects of GDP on microtubule dynamics, due in part to the limited understanding of the true nature of microtubule dynamics and, in particular, of the relationship between the critical concentration, C_c, and the empirical kinetic parameters for microtubule growth and shortening (see Discussion). Also, previous observations of the effects of GDP or Tu-GDP on microtubule dynamics have mostly been done in the presence of MAPs.

In the present work, we have examined the effects of Tu-GDP on tubulin microtubules under conditions of dynamic instability. In this regard, we have assessed the influence of the degree of saturation of the pool of soluble tubulin with GDP on the apparent critical concentration of microtubule assembly, the dynamic length redistribution within the microtubule population, and the rates of growth and shortening of single microtubule ends. The results are discussed in terms of the basic relations between the observable parameters of microtubule dynamics, and they show experimentally that Tu-GDP can alter microtubule dynamics under conditions where the bulk disassembly of microtubules is little affected. This behavior and the striking appearance of irregular microtubule growth in the presence of Tu-GDP are readily simulated within the lateral cap model (Martin et al., 1993) using parameters previously deduced for the interaction of Tu-GDP with microtubule ends. In this model the affinity of Tu-GTP for the microtubule end is postulated to be significantly decreased by the presence of Tu-GDP generated in the terminal layer by previous Tu-GTP hydrolysis. The present work confirms this postulate under conditions where Tu-GDP is introduced as a controlled proportion of the free tubulin concentration. These results thus show how Tu-GDP, or a species acting in an analogous fashion, could act as a potential regulator of microtubule dynamic behavior *in vivo*.

MATERIALS AND METHODS

Materials. MAP-free tubulin was prepared as described (Clark et al., 1981) and was stored at −70 °C in 50 mM Mes buffer, pH 6.5, 0.1 mM EGTA, 7 mM $MgCl_2$, and 3.4

M glycerol. Before each experiment, a suitable sample was assembled and the microtubules were pelleted and resuspended in 100 mM Pipes, pH 6.5, 0.1 mM EGTA, and 1.7 mM $MgCl_2$ (PEM buffer). Alternatively, the microtubules were resuspended in the same buffer containing 1 M glycerol (PEMG). Seeds for seeded-assembly studies were prepared by cross-linking small microtubule fragments with ethylene glycol bis(succinic acid *N*-hydroxysuccinimide ester) (EGS) (Koshland et al., 1988). Seeds were stored at room temperature in PEM buffer (plus 10 mM glutamic acid, 1.5 M sucrose, and 6 mM NaN_3). Prior to each experiment the seeds were sedimented (100000*g*) and resuspended in the appropriate buffer.

GTP and acetyl phosphate were from Sigma Chemical Co.; UTP, UDP, nucleoside-5′-diphosphate kinase (NDPK), and acetate kinase were from Boehringer Mannheim. The purity of UTP was verified by high-performance liquid chromatography (HPLC), and UTP was found to contain 7% UDP. The Bradford reagent was from Bio-Rad Laboratories GmbH.

The concentrations of tubulin and guanosine nucleotides in the samples were calculated from the absorption at 278 and 255 nm with extinction coefficients for tubulin of 1.2 (278 nm) and 0.646 mg^{-1} mL cm^{-1} (255 nm) and values for guanine nucleotide (GDP and GTP) of 7.663 (278 nm) and 12.167 mM^{-1} cm^{-1} (255 nm) (Engelborghs et al., 1993). The concentrations of UTP and UDP stock solutions were determined spectroscopically using an extinction coefficient of 10.0 mM^{-1} cm^{-1} at 262 nm.

Establishing the Fraction of Tu-GDP in Solution. In order to establish a fixed [GDP]/[GTP] ratio in solution, we used the method described by Kristofferson et al. (1982). The concentration of free guanine nucleotide in solution was low, generally some 2.5 times the total tubulin concentration. Under these conditions the [GDP]/[GTP] ratio may be buffered by adding large amounts of UDP and UTP (total [uridine nucleotide] = 1 mM) and 2 units/mL NDPK. The following equilibrium is established by the enzyme:

$$\text{UTP} + \text{GDP} \rightleftharpoons \text{UDP} + \text{GTP}$$

Since the transphosphorylase equilibrium constant of NDPK is unity, the ratio [GDP]/[GTP] equals the ratio [UDP]/[UTP]. If the ratio of the association constants of GTP and GDP for the tubulin E-site is known ($\delta = K_{GTP}/K_{GDP}$), then the [GDP]/[GTP] ratio can be chosen to give the required [Tu-GDP]. On the basis of available information, we have used $\delta = 2.5$ (Carlier & Pantaloni, 1978; Zeeberg & Caplow, 1979; Kristofferson et al., 1982; Fishback & Yarbrough, 1984; Martin & Bayley, 1987).

In addition, a mild GTP-regenerating system was added (0.1 unit/mL AK, 0.5 mM acetyl phosphate) to help overcome the continuous hydrolysis of GTP at the microtubule ends. The effect of acetate kinase on the transphosphorylase system was tested separately. Under the conditions of our experiments, 1 mM UDP is converted to UTP with an initial rate of 2×10^{-3} mM min^{-1}. However, 1 mM UTP is not hydrolyzed to UDP by AK. Therefore, in the presence of NDPK the phosphorylation of UDP by AK together with the phosphorylation of GDP results in the desired regeneration of GTP. Under the experimental conditions, the rate of GDP transphosphorylation is one and one-half times faster. The steady-state hydrolysis of GTP at the microtubule ends was estimated at 3×10^{-3} mM min^{-1} (O'Brien et al., 1987; Melki et al., 1990).

Table 1: Efficacy of the GTP/GDP Coupled Enzyme Buffer

x_D^n	FD_s	FT_s	x_D^r	Δ
0.000	0.114	0.828	0.052	0.052
0.050	0.191	0.704	0.098	0.048
0.100	0.293	0.652	0.152	0.052
0.150	0.328	0.563	0.189	0.039
0.200	0.329	0.547	0.194	-0.006
0.250	0.486	0.457	0.298	0.048
0.300	0.474	0.387	0.329	0.029
0.400	0.573	0.324	0.414	0.014
0.500	0.617	0.223	0.525	0.025

[a] Radioactive GTP was added to the system during the experiment. At the end of the experiment, microtubules were separated from the solution by ultracentrifugation, and the nucleotide composition of the supernatant was determined by HPLC analysis. Typically, each sample was separated into three fractions corresponding to GMP, GDP, and GTP; the solvent front was pooled with the GMP fraction. The fraction of GDP in solution, FD_s, is calculated as [GDP]/([GMP] + [GDP] + [GTP]); the fraction of GTP in solution, FT_s, is calculated as [GTP]/([GMP] + [GDP] + [GTP]). The nominal mole fraction of Tu-GDP, x_D^n, is calculated from the nominal amounts of applied UTP and UDP using a value of $\delta = 2.5$; the "real" mole fraction of Tu-GDP in solution, x_D^r, is given by $1/(1 + \delta FT_s/FD_s)$; $\Delta = x_D^r - x_D^n$.

The performance of the GTP/GDP buffer system was checked by adding radioactively labeled GTP to the system during the experiments. At the end of the experiments, the microtubules were spun down and the nucleotide composition of the supernatant was analyzed by high-performance liquid chromatography [see Martin et al. (1987), Schilstra et al. (1991), and Vandecandelaere et al. (1994)]. The results are given in Table 1. Deviations from the desired level of Tu-GDP were less than 3% when $x_D > 0.25$. However, for low total Tu-GDP percentages the deviation could be as large as 5%. This problem derives in part from the impurity of UTP but, in general, is hard to avoid, as even in the presence of a powerful GTP-regenerating enzyme system, approximately 5% GDP is often found to be present in solution [see, e.g., Schilstra et al. (1991)]. The levels of Tu-GDP that are given in the text and the figures refer to the nominal values based on the added ratio UTP/UDP. In order to check the validity of the results in the presence of UTP ("in the absence" of Tu-GDP), the measurements of the dynamic length redistribution over 60 min and the rate of growth have been repeated under conditions of fast GTP regeneration (1 unit/mL acetate kinase, 2.5 mM acetyl phosphate) in the absence of the NDPK buffer system.

Determination of Apparent Critical Concentration. The effect of Tu-GDP on the critical concentration for assembly was assessed as follows. Phosphocellulose-purified tubulin was assembled at 37 °C in PEM buffer in the presence of NDPK. At steady state, UDP and UTP were added at the different ratios required to establish the desired levels of Tu-GDP. The system was then left to equilibrate for a further 60 min at 37 °C. The microtubules were then sedimented at 100000*g*, and the concentration of protein in the supernatant was determined by Bradford analysis. The concentration of tubulin determined in this manner represents the free dimer concentration in solution at the established total concentration, C_t, of tubulin in the system, and is referred to as the apparent critical concentration, C_c'.

Determination of Microtubule Length Distributions. Samples (typically 5 μL) taken for the determination of length distributions were diluted 10-fold in PEM containing 0.25% glutaraldehyde. After approximately 30 min at room

temperature this solution was diluted 20-fold in PEM. Images of fixed microtubules were taken as soon as possible by dark-field videomicroscopy (Nikon Diaphot microscope and Sony CCD camera) (Bayley et al., 1993). The images were enhanced by integrating 256 frames (Hamamatsu Argus-10 image processor) and were stored for subsequent analysis (software of the Bio-Rad MRC-600 confocal microscope). A typical field contained between 20 and 40 microtubules, and several non-overlapping fields were collected at random for each sample. The lengths of all the microtubules in a single field were measured, providing that microtubule bundling did not make it impossible to discriminate between two or more microtubules. For each sample, between 100 and 200 microtubules were measured in order to construct a length distribution histogram for the population.

Determination of Growth Rates for Individual Microtubules. The effect of Tu-GDP on the growth rate of individual microtubules was measured using dark-field videomicroscopy (Bayley et al., 1994). EGS-cross-linked seeds were prepared as in Koshland et al. (1988). Microtubules were grown on EGS-cross-linked seeds at 37 °C in the presence of the UTP/UDP equilibrating system. EGS seeds were deposited on a clean coverslip and allowed to attach at room temperature. The seeds were then placed in a flow-cell, washed with buffer, and exposed to different mixtures of Tu-GDP/Tu-GTP prior to examination in the microscope. Real-time images were processed by background subtraction and averaging. The enhanced images were stored on S-VHS videotape for subsequent analysis. A length versus time diagram ($L(t)$ plot) was established of single microtubules by sampling the position of the ends with 2−5-s intervals. Phases of growth and shortening and the occurrence of inflection points during growth were distinguished by visual inspection. Growth and shortening rates were determined by application of a straight line through extended portions of monotonous change in the $L(t)$ plot. The in-plane optical resolution was approximately 0.5 μm.

Computer Simulation. The behavior of a *single microtubule* under different solution conditions was simulated using the lateral cap formulation described by Martin et al. (1993). The choice of parameters and formulation of the numerical simulation are discussed under Results.

RESULTS

Unless indicated otherwise, phosphocellulose-purified tubulin (60 μM) was assembled at 37 °C in the presence of 2 units/mL NDPK, 0.1 units/mL AK, and 0.5 mM acetyl phosphate. Fifteen minutes after the start of assembly the solution was divided into separate samples, and the mixture of UDP and UTP (total [uridine nucleotide] = 1 mM) was added as required to establish the desired level of Tu-GDP in solution, x_D (= [Tu-GDP]/{[Tu-GTP] + [Tu-GDP]}). Fifteen minutes later an aliquot from each sample was taken and diluted into 0.25% glutaraldehyde (PEM) for length measurement. The samples were then left to incubate for a further 60 min at 37 °C before a second aliquot for length measurement was collected. The remaining solution was centrifuged at 100000g, and the concentration of protein in the supernatant was determined by Bradford analysis.

In order to measure the effect of Tu-GDP on the dimer exchange in the polymers, controlled amounts of radioactively labeled GTP were added to the system [for details of the method, see Martin et al. (1987), Schilstra et al. (1991), and Vandecandelaere et al. (1994)]. A trace amount of ^{14}C-labeled GTP was added at the start of assembly. Thirty minutes later, a known trace amount of ^{3}H-labelled GTP was added to the samples. The amount of polymer present in the system is deduced from the ^{14}C label, and the ^{3}H label is used to monitor the relative exchange of dimer between the polymeric and the soluble phases. Aliquots for nucleotide analysis were taken 60 min later, and after the centrifugation the nucleotide compositions of the supernatant and the microtubule pellet were also determined. Because this method is based on the analysis of changes in the fractions of [^{14}C]GDP and [^{3}H]GDP in the system, the use of low absolute amounts of GDP is required in order to optimize the signals. The NDPK transphosphorylation buffer was introduced to deal with this requirement.

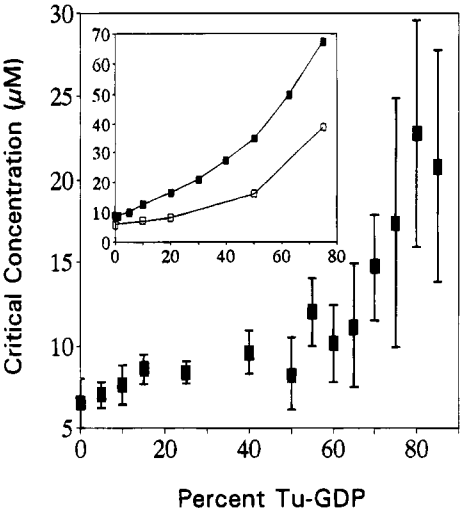

FIGURE 1: Effect of Tu-GDP on the apparent critical concentration for microtubule assembly. The apparent critical concentration, C_c', is shown as a function of the mole fraction of Tu-GDP in solution, x_D, expressed as percent Tu-GDP. The bars give the standard deviation on the mean of four to six measurements. Shown in the inset are the calculated values for the critical concentration for both the α-out (□) and the β-out (■) ends of a 13-protofilament A-lattice. These values are calculated using the lateral cap model for microtubule dynamic instability.

(1) Effect of Tu-GDP on the Apparent Critical Concentration. Figure 1 shows that moderately high levels of Tu-GDP ($x_D \leq 0.5$, 50% Tu-GDP) have only a relatively small effect on the apparent critical concentration, C_c', of the microtubules. Above this value the apparent critical concentration increases in a strongly nonlinear manner. Also shown in Figure 1 is the predicted dependency of the critical concentration, C_c, on [Tu-GDP] according to simulations using the lateral cap formulation for microtubule dynamic instability, details of which are given later (see section 4). C_c is determined by the intercept of the overall growth rate, J_{on}, with the abscissa of a simulated $J_{on}(C)$ plot, i.e., $J_{on}(C_c) = 0$ μm min^{-1}. The qualitative agreement between the simulated behavior and the experimental observations is encouraging.

(2) Effect of Tu-GDP on Microtubule Length Redistribution and Relative Dimer Exchange. The effect of low levels of Tu-GDP ($x_D \leq 0.5$) on the exchange of dimer between the polymer phase and the solution was initially monitored in the presence of 1 M glycerol [cf. Vandecandelaere et al. (1994)]. The analysis of the nucleotide composition of the

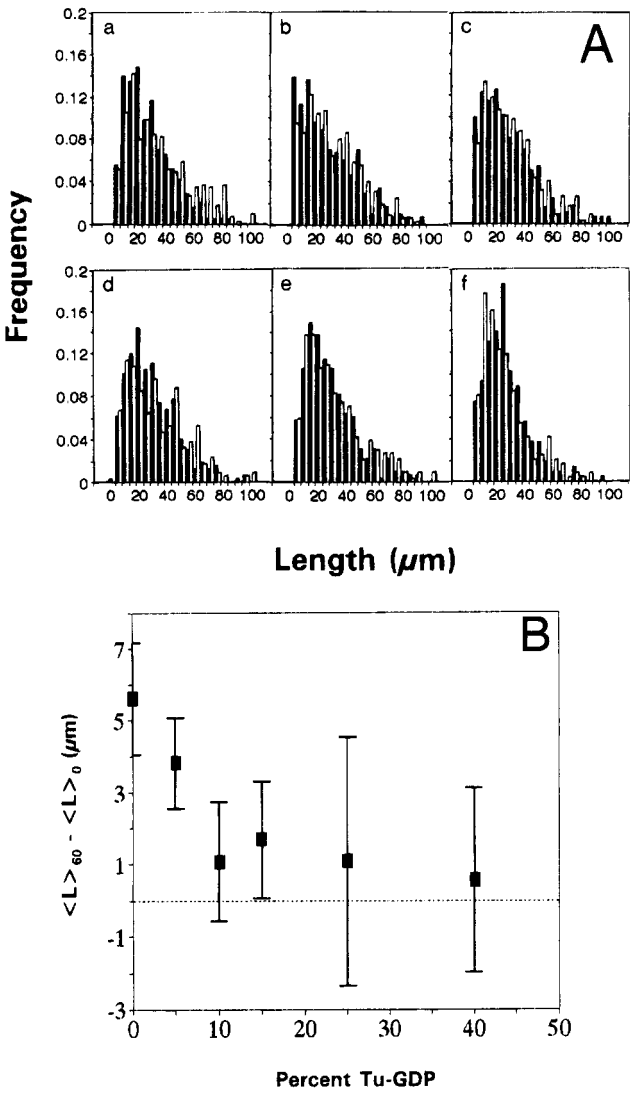

FIGURE 2: Effect of Tu-GDP on the microtubule length redistribution. Samples for length measurement were taken 30 min after the start of assembly (t_0, $\langle L\rangle_0$) and 60 min later (t_{60}, $\langle L\rangle_{60}$) after incubation with Tu-GDP. (A) Length distribution of a microtubule population at time t_0 (filled bars) and at t_{60} (open bars): (a) x_D = 0.00 ($\langle L\rangle_0$ = 25.3 μm; $\langle L\rangle_{60}$ = 33.0 μm); (b) x_D = 0.05 ($\langle L\rangle_0$ = 26.2 μm; $\langle L\rangle_{60}$ = 29.2 μm); (c) x_D = 0.10 ($\langle L\rangle_0$ = 26.7 μm; $\langle L\rangle_{60}$ = 27.4 μm); (d) x_D = 0.15 ($\langle L\rangle_0$ = 27.0 μm; $\langle L\rangle_{60}$ = 29.5 μm); (e) x_D = 0.25 ($\langle L\rangle_0$ = 26.3 μm; $\langle L\rangle_{60}$ = 28.5 μm); (f) x_D = 0.40 ($\langle L\rangle_0$ = 24.0 μm; $\langle L\rangle_{60}$ = 23.3 μm). The histograms have been normalized against the number of measured microtubules in each sample. (B) Change in average length, $\langle L\rangle_{60} - \langle L\rangle_0$, of microtubule populations after 60 min incubation at 37 °C represented as a function of percent Tu-GDP in the solution. The bars give the standard deviation on the mean of at least four measurements.

supernatant showed that the effective level of Tu-GDP in solution ranged from x_D = 0.05 to x_D = 0.53. Within this range the relative exchange of dimers in the microtubules is found to be very small (of the order of 6%) compared with 43% previously found in the absence of GDP (Schilstra et al., 1991). At low levels of exchange the method is not sensitive enough to detect changes in the relative exchange with the variation in mole fraction of Tu-GDP. Therefore, in subsequent experiments, the PEM buffer (without glycerol) was used since it supports a greater dynamic activity.

The effect of Tu-GDP on the length redistribution of the microtubule population is shown in Figure 2A. In conditions of dynamic instability, some of the microtubules in the population, particularly the short ones, may disappear during periods of rapid shortening. As a result the average length, $\langle L\rangle$, of the population tends to increase. The probability of disappearance is high when the average length excursion, ΔL_{avg}, is high. Therefore, the extent to which the average length of the population increases in a fixed period will be high when ΔL_{avg} is high. In Figure 2B the *difference* between the average length of the population after a 1-h incubation at 37 °C ($\langle L_{60}\rangle$) and the corresponding initial average length ($\langle L_0\rangle$) is plotted as a function of percentage Tu-GDP. Tu-GDP suppresses the length redistribution at levels where the effect on the critical concentration (Figure 1) is only moderate. Thus, the average length change is reduced from 5.6 ± 1.6 μm in the absence of Tu-GDP to 0.6 ± 2.5 μm in the presence of 40% Tu-GDP. In the presence of a fast GTP-regenerating system without the NDPK buffer (see Materials and Methods) a change of 6.0 ± 2.1 μm after 60 min was measured, confirming the value measured at 0% Tu-GDP. Although the length histograms (Figure 2A) show significant variability, the effect of Tu-GDP in suppressing the limited length redistribution is clear.

In earlier work the effects of Tu−drug complexes (drug = podophyllotoxin or colchicine) on microtubule dynamics were studied in a buffer containing 1 M glycerol (PEMG) (Schilstra et al., 1989; Vandecandelaere et al., 1994). Although the level of dynamics is reduced in this buffer system (Schilstra et al., 1991), the microtubule ends are still sufficiently dynamic to allow the study of the effects of the Tu−drug complex on the parameters of dynamic instability. The principal advantage of PEMG is that the reproducibility of the initial length distributions is very good, and the resulting experimental variation falls within the limits of variability of a single experiment. In addition, owing to the lower critical concentration in PEMG, the detection limit for nucleotide exchange is reduced. In the present study, glycerol was left out of the buffer in order to increase the level of microtubule dynamics. However, because of the higher level of dynamic instability and the higher critical concentration in PEM, the microtubules are initially much longer than in a glycerol-containing buffer ($\langle L_0\rangle$ = 24.6 ± 5.0 μm in PEM compared with 7.9 ± 2.8 μm in PEMG). Furthermore, the differences between the initial length distributions of otherwise comparable samples are more pronounced than in PEMG, which contributes to an increased experimental variability.

(3) Effect of Tu-GDP on the Growth Rates of Individual Microtubules. Growth rates (R_g) for individual microtubules at 37 °C were determined in dark-field microscopy using small EGS-cross-linked microtubule fragments as seeding structures. The growth rates were measured in PEM buffer for both the fast- and the slow-growing ends of the seeds in the presence of different amounts of Tu-GDP. These measurements were made at one single concentration of tubulin in solution, C_s well above C_c', because at the steady state the effect of a high level of Tu-GDP (x_D > 0.15) is to reduce the average length excursion of the growing phases to the point where accurate measurements of R_g are no longer possible. This approach assumes that the effect of Tu-GDP on R_g at C_s can be extrapolated to the steady state. This was confirmed by measurements at the approximate C_c' for $0 \le x_D \le 0.15$ (results not shown). Microtubule growth of the fast-growing end is illustrated in Figure 3A; the exact conditions are indicated in the legend. Length is plotted

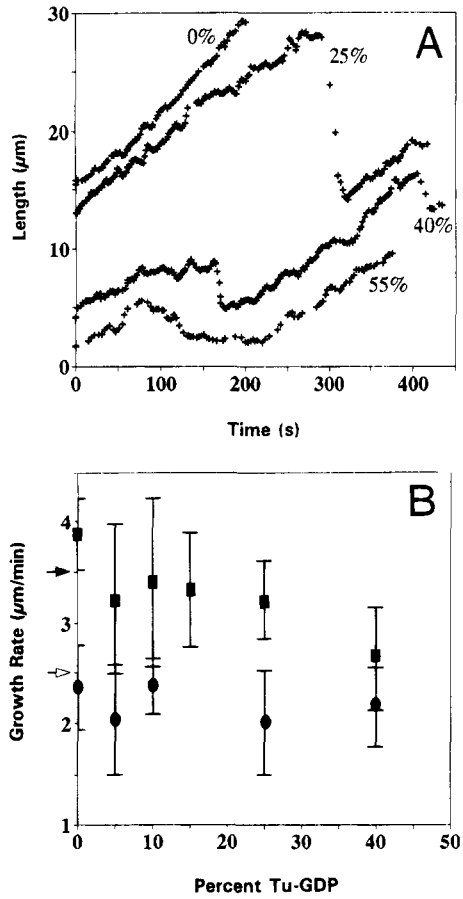

FIGURE 3: Experimental observation of the effect of Tu-GDP on microtubule growth. (A) Length versus time plots of the fast-growing ends of a microtubule. Growth of EGS-cross-linked microtubule fragments was monitored by dark-field videomicroscopy at 37 °C. The concentration of tubulin, C_t, was 14.3 μM (upper three curves) or 17.7 μM (lower curve), and the solutions contained in descending order 0%, 25%, 40%, and 55% Tu-GDP. The curves have been translated along the ordinate to avoid overlap. At higher levels of Tu-GDP ($x_D > 0.4$) the behavior of the two ends of a single microtubule is similar, and the assignment of the ends becomes ambiguous. (B) Measured growth rates, R_g, as a function of percent Tu-GDP at $C_t = 14.3$ μM. Values of R_g are given for the fast-growing end (■) and the slow-growing end (●). The bars give the observed variation in R_g, irrespective of whether these values are observed in a single microtubule or in the microtubule population. The arrows indicate the growth rate of the fast-growing (solid arrowhead) and the slow-growing ends (open arrowhead) in the presence of a fast GTP-regenerating enzyme system (see text).

versus time for the fast-growing end in the absence and presence of 25%, 40%, and 55% Tu-GDP. Both ends of a single microtubule were measured, and the discrimination between the fast- and the slow-growing ends was based on the measured rates. At higher levels of Tu-GDP the rates for the two ends are similar, and their assignment becomes ambiguous, even if the size of the length changes during single excursions of growth or shortening is included in their assignment. [For a discussion of the intrinsic ambiguity in assigning the fast- and slow-growing ends, see Kowalski and Williams (1993).]

The data indicate that an increased saturation of tubulin with GDP affects the rates during periods of growth in a rather subtle manner. Figure 3B shows the values of the growth rate as a function of percent Tu-GDP (measured at $C_t = 14.3$ μM) for the two ends of single microtubules. Under the conditions employed, Tu-GDP has a more significant effect on the growth rate for the fast-growing end, $R_{g,f}$. At 14.3 μM total tubulin $R_{g,f} = 3.9 \pm 0.4$ μm/min in the absence of Tu-GDP and 2.6 ± 0.5 μm min^{-1} in the presence of 40% Tu-GDP. The growth rate of the slow-growing end, $R_{g,s}$, remains at 2.3 ± 0.5 μm min^{-1} throughout. Again, the value measured for 0% Tu-GDP was checked by performing the same experiment in the presence of a fast GTP-regenerating system without the NDPK buffer (see Figure 3B). The following values were measured: $R_{g,f} = 3.5 \pm 0.4$ μm min^{-1} for the fast-growing end, and $R_{g,s} = 2.5 \pm 0.3$ μm min^{-1} for the slow-growing end. This result indicates that the values are not affected by the presence of traces of UDP in the UTP product. Although Tu-GDP does not affect the value of $R_{g,f}$ very much, comparing, for example, growth in 40% Tu-GDP with growth in the absence of Tu-GDP in Figure 3A reveals decreased *regularity* of growth with increasing levels of Tu-GDP. Thus, in the presence of 40% Tu-GDP, $R_{g,f}$ was found to range from 1.4 to 3.3 μm min^{-1} for the illustrated end during a single excursion of growth (excluding the pause; see below). In the absence of Tu-GDP, such variation in $R_{g,f}$ was not observed for growth of a single microtubule end but does exist in the population of growing ends. The data in Figure 3B incorporate all the variations seen in R_g, including those in the length versus time plot of a single microtubule. The intrinsic irregularity of microtubule growth has been reported before (Gildersleeve et al., 1992); this irregularity is clearly enhanced by Tu-GDP.

As illustrated in Figure 3A, the probability of observing transitions from the growing to the shortening state (G → S) increases with increasing levels of Tu-GDP, even at concentrations significantly above C_c. Also, pause periods during which little or no net growth (or shortening) is observed become more frequent at higher percentages of Tu-GDP (illustrated at 40% Tu-GDP, $C_t = 14.3$ μM). Furthermore, particularly when a high concentration of tubulin is combined with a high saturation with GDP, phases of remarkably slow shortening can also be observed (illustrated at 55% Tu-GDP, $C_t = 17.7$ μM). These observations illustrate the complicated nature of the rates of growth and shortening, which both reflect a balance between addition and dissociation reactions of dimers to the microtubule lattice. Because the amplitudes of the phases of shortening (Figure 3A) are rather brief in time and small in length, only a low number of points are sampled during shortening. Hence, the rates during shortening of microtubules in these conditions are only poorly defined. Measurements of shortening rates of, e.g., the fast-growing ends gave values of 16−33 μm min^{-1} for $x_D = 0.1-0.4$, and within the limits of accuracy in our optical system no obvious dependence of R_s on x_D was observed. A combined rate of shortening was calculated for the fast-growing end ($R_{s,f} = 25 \pm 8$ μm min^{-1}) and for the slow-growing end ($R_{s,s} = 15 \pm 8$ μm min^{-1}).

No attempt was made to estimate the transition frequencies, T_g^{-1} and T_s^{-1}, for the following reasons: (1) A single microtubule may not be representative of the entire population. Therefore, an unrealistically large number of observations of transitions of a single end would be required to produce reliable estimates of the average lifetimes for growth, T_g, and shortening, T_s [see Bayley et al. (1991)]. (2) Both T_g and T_s depend in a sensitive nonlinear manner on the dimer concentration in solution (Walker et al., 1991; Bayley et al., 1994). Therefore, significant experimental uncertainties in the value of C_c would make it difficult to assess the effect

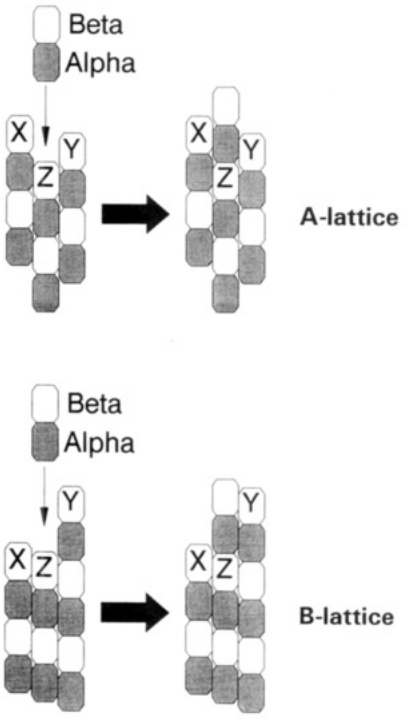

FIGURE 4: Addition of a tubulin $\alpha\beta$-heterodimer to the microtubule lattice according to the lateral cap formu tion for microtubule dynamic instability. The β-out end of the 1 protofilament A-type and B-type lattices are shown in part (s ading, α-subunit; no shading, β-subunit). A typical site of ad ition is given by the configuration XZY. The affinity of the $\alpha\beta$- eterodimer for this site is a function of the nature of the nucleo de (GTP or GDP) on β-subunits X and Y. The affinity for the sites in ascending order is DD < DT $\approx$ TD < TT, with T for GTP and D for GDP. Upon addition of the dimer, GTP on subunit Z is hydrolyzed [see Figures 1 and 2 in Martin et al. (1993)].

of Tu-GDP on the transition frequencies. However, the combined effect of Tu-GDP on the critical concentration, the dynamic length redistribution, and the rates of growth and shortening yields valuable information on the effect of Tu-GDP on the transition frequencies (see Discussion).

(4) Numerical Simulation of the Effect of Tu-GDP on Microtubule Dynamic Instability. A generalized numerical model employing Monte Carlo methods has been developed to treat the dynamic behavior of microtubule ends, based on the lateral cap formulation for microtubule dynamic instability (Bayley et al., 1990). In the current version of the model [for details, see Martin et al. (1993)], the free energy changes associated with the interactions of each individual subunit with its neighbors in the lattice are considered. This approach permits the treatment of the interaction of a subunit with microtubule lattices of any specified symmetry, and for binding at either end of the microtubule. From the sum of the partial free energy changes upon incorporation in the lattice, the corresponding affinity of a subunit for any particular site in the lattice is deduced. Dissociation rate constants are calculated from these affinities, using specific assumptions about the association rate constants (see below). The addition of a dimer in solution to a site in the microtubule end is illustrated in Figure 4, which shows part of the β-out end of the 13-protofilament A- and B-lattices. A typical site of addition is given by the configuration XZY. The affinity of a dimer for this site depends on the number of interactions with adjacent subunits and the nature of the nucleotide (GTP or GDP) on the E-site of the neighboring

Table 2: Rate Constants for the Dissociation of Tu-GTP and Tu-GDP from Four Different Sites at the α- and β-Out Ends of the 13-Protofilament A-Lattice[a]

	β-out end		α-out end	
site (XY)	$k_{-,T/XY}$ (s^{-1})	$k_{-,D/XY}$ (s^{-1})	$k_{-,T/XY}$ (s^{-1})	$k_{-,D/XY}$ (s^{-1})
TT	2.0	10.8	10.2	200.0
TD	17.6	51.2	20.6	222.2
DT	22.8	75.4	26.8	333.4
DD	200.0	363.6	54.8	363.6

[a]The association constants of Tu-GTP, $K_{T/XY}$, and Tu-GDP, $K_{D/XY}$, for the specified sites are calculated from six free energy difference terms and are given in Table 2 in Martin et al. (1993). Here, the association rate constant, $k_{+,XY}$, is assumed to be identical for Tu-GTP and Tu-GDP and independent of the nature of the nucleotides in positions X and Y (see Figure 4): $k_{+,T/XY} = k_{+,D/XY} = 2 \times 10^6$ M^{-1} s^{-1}. The dissociation rate constants are calculated as $k_{-,T/XY} = k_{+,T/XY}/K_{T/XY}$ and $k_{-,D/XY} = k_{+,D/XY}/K_{D/XY}$.

subunits X and Y. The affinity is highest if the nucleotides on both subunits X and Y are GTP (shorthand notation: TT-site), and it is lowest with X and Y containing GDP (DD-site), with intermediate affinities for the TD- and DT-sites. What distinguishes the lateral cap model from other models [e.g., Chen and Hill (1985)] is its postulate that GTP on subunit Z is hydrolyzed upon the addition of any dimer to the site XZY. With these postulates and assumptions it is possible to simulate the dynamic behavior of a microtubule end by computer calculation for all lattice types.

The purpose of the simulation is to see how the concepts of the detailed model are able to reproduce the type of behaviour observed experimentally. In view of the experimental uncertainties in determining the absolute values of observable quantities characterizing microtubule dynamics, this study does not attempt a refinement of the input parameters of the model to seek a precise numerical fit to a set of experimental data. In the present work, the calculations have been performed on the 13-protofilament microtubule A-lattice. The input parameters for the simulation are the set of site dissociation rate constants, $k_{-,T/XY}$ and $k_{-,D/XY}$, calculated from the site affinities, $K_{T/XY}$ and $K_{D/XY}$. These affinities derive in turn from only six free energy difference terms [see Table 2 in Martin et al. (1993)]; the site association rate constant, $k_{+,XY}$, was set at 2×10^6 M^{-1} s^{-1} irrespective of the nature of the nucleotide on the dimer being added, or in other words, it is assumed that $k_{+,T/XY} = k_{+,D/XY}$. The resulting site dissociation rate constants are given in Table 2. This self-consistent treatment indicates that although the affinity of Tu-GDP for a DD-site at both the α-out and the β-out end is low (resulting in a high value for $k_{-,D/DD} \approx 364$ s^{-1}), this affinity is significantly higher if the neighboring subunits contain E-site GTP (e.g., for the β-out end: $k_{-,D/TT} = 11$ s^{-1}, $k_{-,D/TD} = 51$ s^{-1}, $k_{-,D/DT} = 75$ s^{-1}). In addition, the affinity of Tu-GDP for T-containing lattice sites in the β-out end is of a similar order of magnitude to the affinity of Tu-GTP for similar sites.

The simulation for a particular end consists of the construction of a plot of growth rate as a function of tubulin concentration [$J_{on}(c)$] [see Martin et al. (1993)]. The critical concentration, C_c, is derived from the intercept with the abscissa in such a $J_{on}(c)$ plot. The changes of the calculated critical concentration with percent Tu-GDP are shown in Figure 1 for both the α-out and the β-out end of the 13-protofilament A-lattice. As mentioned above, no quantitative similarity with the observations was aimed at. Nevertheless,

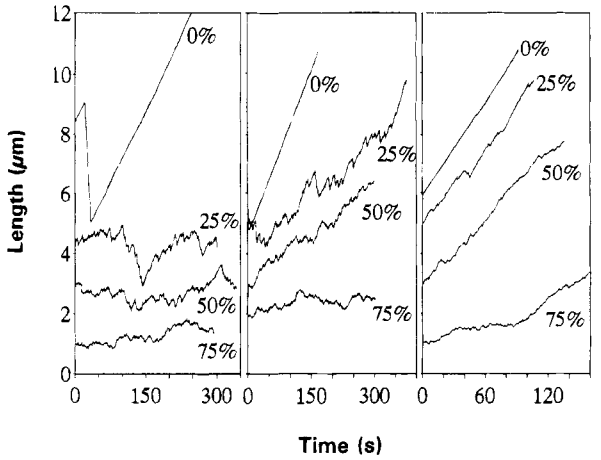

FIGURE 5: Simulation of the effects of Tu-GDP on microtubule dynamics. Computer simulations were based on the lateral cap formulation for microtubule dynamic instability (cf. Figure 4) and were performed on the 13-protofilament A-lattice. The effects of Tu-GDP on the length changes of the β-out end at steady state (left panel), at $C_s = C_c + 1$ μM (middle panel), and at $C_s = C_c + 5$ μM (right panel) are shown. From top to bottom Tu-GDP ranges are $x_D = 0.00$ ($C_c = 8.25$ μM), $x_D = 0.25$ ($C_c = 19$ μM), $x_D = 0.50$ ($C_c = 35.2$ μM), and $x_D = 0.75$ ($C_c = 67.7$ μM). The curves have been translated along the ordinate to avoid overlap.

Figure 1 demonstrates a good agreement of the observed dependence of the apparent critical concentration on Tu-GDP with the calculations of the model. According to the lateral cap model, the response of both microtubule ends to elevated levels of Tu-GDP is similar, with the β-out end more sensitive, and the change in the critical concentration is moderate up to $x_D = 0.5$. Thus, only at high percentages of Tu-GDP in solution does the microtubule polymer mass become significantly dependent on x_D. However, low levels of Tu-GDP are predicted to significantly affect the dynamic behavior of the microtubule ends (see below).

Figure 5 shows the calculated effects of Tu-GDP on the dynamics of the β-out end. The length versus time diagram clearly indicates that Tu-GDP causes a remarkable suppression of the average length excursions during growth and shortening. These simulations were performed both at steady state of assembly and in conditions of growth, i.e., $C_s > C_c$; note the increase of C_c with Tu-GDP. In all cases, growth and shortening become highly irregular in the presence of Tu-GDP, and especially considering the increase of C_c, Tu-GDP causes a significant reduction of the overall growth rate. Under certain conditions of C_s and x_D, "pause" periods of no net length change are observed, although addition and dissociation of dimers to the end still occur with high frequency. Finally, at high levels of Tu-GDP it is no longer possible to characterize the dynamics of the end at steady state in terms of the parameters of a two-phase system. Figure 6A shows the effect of Tu-GDP on the growth rate, R_g, of the α-out and β-out ends at a constant C_s well above C_c. The results are presented relative to the value of R_g in the absence of Tu-GDP. In agreement with the results in Figure 3B, only a small reduction of R_g by moderate levels of Tu-GDP is predicted. Figure 6A indicates that the effects on R_g become progressively greater at higher levels of Tu-GDP. This is mainly due to the effect on R_g of the increased contribution of dissociation events. The different response of the ends is related to the fact that the two ends have different critical concentrations. Figure 6B shows the effect of moderate levels of Tu-GDP on the average lifetime of

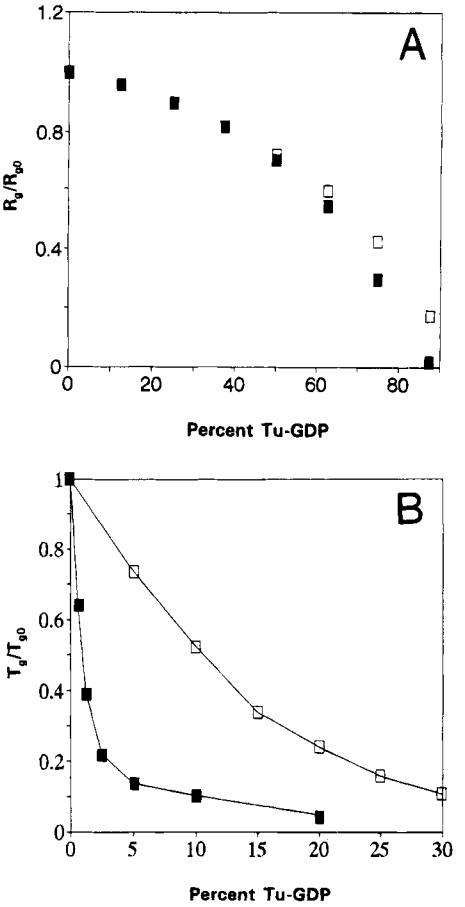

FIGURE 6: Calculated effects of Tu-GDP on the growth rate, R_g, and the lifetime of growth, T_g. (A) Effect of Tu-GDP on the growth rate, R_g, of the α-out and β-out ends. Rates are expressed relative to the rate of growth in the absence of Tu-GDP, R_{g0}. The total concentration of tubulin in solution was kept constant at 100 μM; $R_{g0}^{\alpha} = 24.5$ μm min^{-1}, and $R_{g0}^{\beta} = 25.2$ μm min^{-1}. (B) Effect of Tu-GDP on the average time of growth, T_g, of both the α-out (□) and the β-out ends (■) at steady state. Again, values of T_g are expressed relative to the value in the absence of Tu-GDP, T_{g0}; $T_{g0}^{\alpha} = 0.55$ min, and $T_{g0}^{\beta} = 2.13$ min. Note the strong dependence of T_g on very low levels of Tu-GDP.

the growth phase, T_g, of both the α-out and the β-out ends. Although low levels of Tu-GDP do not significantly affect the critical concentration and the growth rates, T_g is strongly affected in this range. In particular, the dynamic properties of the β-out end are strongly affected by Tu-GDP. The significant reduction of the dynamic length changes by low levels of Tu-GDP shown in Figure 2 supports this prediction of the simulation. Thus, despite the fact that few macroscopic changes can be observed, the lateral cap model predicts a sensitive dynamic response of the microtubule ends in the low Tu-GDP range, with a dramatic reduction of the lifetime of the growing state, T_g, and, consequently, a reduction of the average length excursions, ΔL_{avg}.

DISCUSSION

(1) Effect of Tu-GDP on Empirical Parameters of Microtubule Dynamic Instability. Regardless of the choice of model for the molecular mechanism of microtubule dynamic instability, the population behavior of microtubules undergoing simple two-state behavior can be described by four empirical parameters at any tubulin concentration, C_t: the mean rates of growth and shortening (R_g and R_s) and the mean lifetimes of the growing and shortening states (T_g and

T_s) (Bayley et al., 1989). The effect of any agent can be investigated in terms of its influence on each of these parameters. At steady state of assembly, the polymer is in equilibrium with free tubulin (the critical concentration C_c) and $R_gT_g = R_sT_s$. The behavior of a single microtubule *over long times* may be described by the same growth and lifetime parameters. The average length excursion, ΔL_{avg}, during periods of growth and shortening is given by R_gT_g for growth and R_sT_s for shortening. At steady state of assembly,

$$\Delta L_{avg} = R_gT_g = T_sT_s \quad (1)$$

In this equation R_g represents a combination of the growth rates, $R_{g,f}$ and $R_{g,s}$, of the fast-growing and slow-growing ends of a single microtubule. Similarly, R_s is given by the combination of the rates of shortening of both ends of a single microtubule. Observed values for R_g and R_s represent a balance between addition and dissociation events, and therefore, observed rates of growth and shortening may not always be a reflection of the empirical rate constants k_{on} and k_{off} for addition and loss of dimer as defined by generalized kinetic equations [e.g., Walker et al. (1988), O'Brien et al. (1990), Pryer et al. (1992), and Simon et al. (1992)]. Thus, only in conditions where all soluble tubulin is Tu-GTP and the dissociation of dimer can be neglected, i.e., at $C_t \gg C_c$, can an optimal observable growth rate be defined as $R_g^{opt} = C_tk_{+T/TT}n = C_tk_{on}$, where $k_{+T/TT}$ is the site-specific association rate constant for Tu-GTP (Figure 4), and n is the average number of association sites in the microtubule end. Similarly, a maximal observable shortening rate can be defined by $R_s^{opt} = k_{-D/DD}n$ (Bayley et al., 1990). At steady state of assembly, i.e., $C_t = C_c$, expressions for R_g and R_s adopt a more complex format reflecting the balance between association and dissociation events and the average mixed composition of a microtubule end. Since the average composition of a microtubule end is different during phases of growth and shortening, and since at steady state growth and shortening are interconnected through eq 1, the critical concentration, C_c, cannot be expressed as a ratio of two rate constants (k_{off}/k_{on}) as is the case for a condensation homopolymer (Oosawa & Asakura, 1975).

In agreement with many previous observations (Carlier & Pantaloni, 1978; Zackroff et al., 1980; Kristofferson et al., 1982), low to moderate levels of Tu-GDP do not have a major effect on the apparent critical concentration of tubulin microtubules. Saturating 60% of the soluble tubulin with GDP increases C_c' by a factor of 1.5, from 6.5 to 10.1 μM (Figure 1). Tu-GDP also has a rather limited effect on the rates of growth and shortening. Significant effects on the rate of shortening were only observed at high total tubulin concentrations with very high levels of GDP saturation. The growth rate for the fast-growing end is reduced in the presence of Tu-GDP; the rate for the slow-growing end is not affected (by up to 40% Tu-GDP). In contrast, Tu-GDP does have an appreciable effect on the extent of microtubule length redistribution (Figure 2). Saturation of 40% of the tubulin dimer with GDP is sufficient to abolish dynamic length changes. This implies that the average length excursions (ΔL_{avg}) must be greatly reduced in the presence of Tu-GDP. Within the limits of our observations, values for the rate of growth slightly above C_c' show linear dependence on the concentration of tubulin in solution. Therefore, the moderate effect of Tu-GDP on the observed growth rates (Figure 3B) suggests that the reduction of ΔL_{avg} derives from a decrease in lifetimes (T_s and T_g) rather than in rates (R_s and R_g).

The observations in dark-field microscopy reveal an increased occurrence of G $\rightleftharpoons$ S transitions with increasing GDP saturation, even under conditions well above C_c'. Furthermore, the likelihood of microtubule ends entering a pause state, i.e., a state during which no pronounced net growth or shortening occurs, is seen experimentally to increase with Tu-GDP (Figure 3A). In addition, at higher Tu-GDP levels the individual growth phases become more irregular and display a wider range of growth rates. Typically, for the fast-growing end in the absence of Tu-GDP little variation in $R_{g,f}$ for a single microtubule is observed, although a fairly wide range of values for $R_{g,f}$ exists within the microtubule population ($\langle R_{g,f} \rangle = 3.9 \pm 0.4$ μm min^{-1} at 14.3 μM in the absence of Tu-GDP). However, at 40% Tu-GDP in otherwise similar conditions $R_{g,f}$ was found to range from 1.4 to 3.3 μm min^{-1} for a single microtubule end during a period of continuous growth. These phenomena can be understood in terms of the increased frequency of G $\rightleftharpoons$ S transitions in the presence of Tu-GDP. As a result of the reduction of the average lifetimes (T_g and T_s), the average excursions of growth, $\Delta L_{avg,g}$ (= R_gT_g), and of shortening, $\Delta L_{avg,s}$ (= R_sT_s), are reduced and can be expected to fall below the optical resolution of the microscope under certain conditions of tubulin concentration and GDP saturation. Under these conditions, T_g and T_s cease to be observable parameters and simply represent the average times between the addition and the dissociation of a small number of dimers.

(2) Mechanism of Interaction of Tu-GDP with the Microtubule Lattice. Previous treatments of the effects of Tu-GDP (or GDP) on microtubule assembly properties fall into three main classes (Kristofferson et al., 1982): (1) The Tu-GDP present simply constitutes a pool of inactive tubulin which does not participate (significantly) in the addition reactions [e.g., Jameson and Caplow (1980), and Bayley and Martin (1986)]. (2) Tu-GDP does support microtubule elongation but with a reduced association rate constant [e.g., Carlier and Pantaloni (1978), and Kristofferson et al. (1982)]. (3) Tu-GDP does not support elongation but nevertheless binds to the microtubule ends and stabilizes them [e.g., Zackroff et al. (1980), and Caplow and Reid (1985)]. At the time when these models were formulated, little was known about the nature of microtubule dynamics. In the meantime, it has been shown that Tu-GDP binds to the microtubule end with an apparent dissociation constant of 5.5 μM in the absence of MAPs and in a buffer containing 3.4 M glycerol (Carlier et al., 1987b), suggesting that the affinity of Tu-GDP for the microtubule ends (in these conditions) is only 1 order of magnitude lower than the affinity of Tu-GTP for such ends.

In this work, the lateral cap model for dynamic instability (Martin et al., 1993; Bayley et al., 1994) has been used to simulate the effects of Tu-GDP on the dynamics of the β-out end of the 13-protofilament microtubule A-lattice (Amos, 1979). For the details of the model the reader is referred to Martin et al. (1993) or Bayley et al. (1994). Briefly, the affinity for well-defined sites in the microtubule lattice is calculated from free energy values which depend on the number of interactions with adjacent subunits and the nature of the nucleotide (GTP or GDP) on the E-site of the neighboring subunits (see Figure 4). Thus, the affinity of

any dimer (Tu-GTP or Tu-GDP) for the site XZY in Figure 4 is highest if the nucleotides on both subunits X and Y are GTP (shorthand notation: TT-site), and it is lowest with X and Y containing GDP (DD-site), with intermediate affinities for the TD- and DT-sites. Upon addition of a dimer to the site XZY, GTP on subunit Z is hydrolyzed. The addition of Tu-GTP to the lattice may create a new addition site which can be either TT, TD, or DT, whereas the addition of Tu-GDP creates a DT-, a TD-, or a DD-site. Assuming that the intrinsic association rate constant, $k_{+,XY}$, for any site XY is the same for Tu-GTP or Tu-GDP at any site XY, one can calculate the dissociation rate constant, $k_{-,XY}$, of each dimer in the lattice from its affinity. This dissociation rate constant is highest if XY is DD and lowest if XY is TT.

In the most general treatment of the lateral cap model (Martin et al., 1993), it was deduced that the affinity of Tu-GDP for the TT-site of the β-out end of a microtubule should be relatively high (e.g., about one-fifth that of Tu-GTP for a TT-site) compared with the low affinity for Tu-GTP at a DD-site. This suggests that Tu-GDP should have specific and observable effects on microtubule dynamics, a prediction which is confirmed in this work. Further, the addition of Tu-GDP causes the hydrolysis of previously terminal GTP-containing subunits, as well as creating new sites with reduced affinity in which the Tu-GDP is the X or Y neighbor. Consequently, the probability for a G → S transition to occur is increased. Thus, according to the lateral cap model, Tu-GDP modifies the composition of the microtubule ends in a most subtle manner. On average, the number of high-affinity TT addition sites is reduced by the addition of Tu-GDP. At steady state, this condition increases the likelihood for shortening; hence the requirement for a higher number of addition events or, in other words, a higher critical concentration. An indication that the composition of at least one microtubule end is modified in the presence of Tu-GDP was provided by the work of Engelborghs and Van Houtte (1981).

The combination of the evidence from Figures 1, 2, and 3 indicates that the principal effect of Tu-GDP is on the transition frequencies. The lateral cap model rationalizes how the presence of Tu-GDP favors transitions from the growing to the shortening state and hence reduces T_g. As a consequence of the increased number of G → S transitions, more dimers are released into solution; hence a higher apparent critical concentration in the presence of Tu-GDP. However, the increase in soluble tubulin concentration results in an increased number of addition events. As a result, the likelihood for S → G transitions also increases. This leads to a reduction of T_s. If C_c' were kept constant at its original value in the absence of Tu-GDP, an increased likelihood of G → S transitions by Tu-GDP would result in complete disassembly of the microtubule: the lower affinity of dimers for Tu-GDP-containing association sites in the microtubule end would not support a sufficiently high number of addition reactions to compensate for the increased likelihood of dimer loss. Tu-GDP by itself does not favor the occurrence of S → G transitions, but given its finite affinity for the microtubule lattice, it does participate with Tu-GTP in addition reactions which may lead to such a transition. Therefore, the reduction of T_s by Tu-GDP must be regarded as secondary to the effect of increasing C_c'. In general, T_s and T_g are not affected in a similar manner. It is not possible to confirm whether Tu-GDP has specific inhibitory effects on microtubule growth in addition to its effects on the transition frequencies. A reduction in R_g with Tu-GDP may reflect a slight inhibition of growth by Tu-GDP (as implied by the reduced affinity of dimer for GDP-containing binding sites in the microtubule end), but it may also represent an increased number of dissociation events relative to the number of addition reactions. The dependence of R_g on x_D as predicted in Figure 6A derives principally from the increased contribution of dissociation events to R_g. This is mainly due to a reduction in the number of high-affinity TT-sites and a corresponding increase in the number of low-affinity DT-, TD-, and DD-sites. This effect becomes progressively more important at higher values of x_D (see also Table 2). The similarities between the predictions of Figure 6A and the observations of Figure 3B for the range $0 \leq x_D \leq 0.40$ suggest that the effect of Tu-GDP can be attributed to this mechanism. During shortening, too, addition reactions occur, and their contribution can become significant. An illustration of the latter effect is given by periods of slow disassembly at high levels of GDP saturation and high concentrations of tubulin (Figure 3A).

It should be emphasized that the lateral cap model provides a kinetic scheme for the numerical treatment of the dynamic behavior of single microtubule ends. As such it does not define the specific molecular mechanisms involved in microtubule dynamics. Thus, e.g., the present formulation does not necessarily exclude the possibility of conformational changes of subunits during association or dissociation reactions (Howard & Timasheff, 1986; Melki et al., 1989; Shearwin & Timasheff, 1992; Shearwin et al., 1994; Díaz et al., 1994). Providing that such processes are not rate-determining steps, no additional rate constants are required in the model. Implied in the assumptions of the model is the concept that lateral interactions between GDP-containing subunits in the lattice are generally weaker than the corresponding lateral interactions between GTP-containing subunits, whether these distinctions are caused by differences in the intrinsic conformations of Tu-GDP and Tu-GTP [e.g., Melki et al. (1989), and Díaz et al. (1994)] or by other structural factors. In addition, modeling based on free energy considerations (Martin et al., 1993) shows that variations in the microtubule lattice can produce significant differences in kinetic properties; e.g., the 14-protofilament A-lattice grows and shortens more slowly than the 13-protofilament A-lattice. However, variations in protofilament number appear to be infrequent (Chrétien et al., 1992) and may contribute only to long-term changes in observed growth rates. For convenience the simulations have been performed using the fully symmetric 13-protofilament A-lattice. Recent evidence indicates that the B-type lattice is present in microtubules of brain tubulin and the A- and B-tubules of flagellar outer doublets (Song & Mandelkow, 1993). In fact, the uniqueness of the symmetry of the microtubule lattice remains an open question. The occurrence of a wide variation in the microtubule protofilament number within a population after self-assembly implies the coexistence of different lattice type contacts, and hence suggests that thermodynamic differences between the different types of lattice interactions are small. Therefore, a mixture of A- and B-type lattice contacts may well be present in both single microtubules and the microtubule population. Short-term irregularities in microtubule growth have been observed by Gildersleeve et al. (1992). These might correspond to

changes of lattice symmetry, although the simulations in Figure 5 show that irregularities are readily reproduced for a single lattice type by the lateral cap model.

In summary, the principal effect of Tu-GDP on microtubule dynamic instability is deduced to be an increase of the frequency of the transitions between the phases of growth and shortening. With increasing levels of Tu-GDP in solution, microtubule dynamics cease to conform to a simple two-phase process. Growth and shortening become more irregular, and on average, the length excursions of the microtubule ends are reduced. According to the lateral cap model, the addition of Tu-GDP to the lattice can only create new addition sites of the type TD, DT, or DD, and on average the number of highest affinity TT-sites per end is reduced. The experimental data are well reproduced by computer simulations based on this model. In view of its interactions with the microtubule ends, Tu-GDP seems to be a potential endogenous regulator of microtubule dynamics, whose effects would be dependent on Tu-GTP/Tu-GDP concentrations in the vicinity of a microtubule end. More generally, as previously deduced for the effect of tubulin−drug complexes (Vandecandelaere et al., 1994), the binding to the microtubule end of a factor which decreases the subsequent affinity for tubulin dimer can have the effect of suppressing dynamic length changes in a sensitive manner.

ACKNOWLEDGMENT

We thank Marietje Schilstra and Yves Engelborghs for helpful discussions.

REFERENCES

Amos, L. A. (1979) in *Microtubules* (Roberts K., & Hyams, J. S., Eds.) pp 1−64, Academic Press, London.

Audenaert, R., Heremans, L., Heremans, K., & Engelborghs, Y. (1989) *Biochim. Biophys. Acta 996*, 110−115.

Bayley, P. M., & Martin, S. R. (1986) *Biochem. Biophys. Res. Commun. 137*, 351−358.

Bayley, P. M., Butler, F. M. M., & Manser, E. J. (1986) *FEBS Lett. 205*, 230−234.

Bayley, P. M., Schilstra, M. J., & Martin, S. R. (1989) *J. Cell Sci. 93*, 241−254.

Bayley, P. M., Schilstra, M. J., & Martin, S. R. (1990) *J. Cell Sci. 95*, 33−48.

Bayley, P. M., Martin, S. R., & Sharma, K. K. (1991) *AIP Conf. Proc. 226*, 187−199.

Bayley, P. M., Martin, S. R., & Schilstra, M. J. (1993) *Cell. Pharmacol. 1* (Suppl. 1), 551−556.

Bayley, P. M., Sharma, K. K., & Martin, S. R. (1994) in *Microtubules* (Hyams, J., & Lloyd, C., Eds.) pp 111−137, Wiley-Liss, New York.

Bergen, L. G., & Borisy, G. G (1982) *J. Biol. Chem. 258*, 4190−4194.

Berry, R. W., & Shelanski, M. L. (1972) *J. Mol. Biol. 71*, 71−81.

Caplow, M., & Reid, R. (1985) *Proc. Natl. Acad. Sci. U.S.A. 82*, 3267−3271.

Carlier, M.-F., & Pantaloni, D. (1978) *Biochemistry 17*, 1908−1915.

Carlier, M.-F., & Pantaloni, D. (1981) *Biochemistry 20*, 1918−1924.

Carlier, M.-F., Melki R., Pantaloni, D., Hill, T. L., & Chen, Y. (1987a) *Proc. Natl. Acad. Sci. U.S.A. 84*, 5257−5261.

Carlier, M.-F., Didry, D., & Pantaloni, D. (1987b) *Biochemistry 26*, 4428−4437.

Chen, Y., & Hill, T. L. (1985) *Proc. Natl. Acad. Sci. U.S.A. 82*, 1131−1135.

Chrétien, D., Metoz, F., Verde, F., Karsenti, E., & Wade, R. H. (1992) *J. Cell Biol. 117*, 1031−1040.

Clark, D. C., Martin, S. R., & Bayley, P. M. (1981) *Biochemistry 20*, 1924−1932.

Correia, J. J., Baty, L. T., & Williams, R. C. (1987) *J. Biol. Chem. 262*, 17278−17284.

Díaz, J. F., Pantos, E., Bordas, J., & Andreu, J. M. (1994) *J. Mol. Biol. 238*, 214−223.

Drechsel, D. N., Hyman, A. A., Cobb, M. H., & Kirschner, M. W. (1992) *Mol. Biol. Cell 3*, 1141−1154.

Dustin, P. (1978) *Microtubules*, Springer-Verlag, Berlin.

Engelborghs, Y., & Van Houtte, A. (1981) *Biophys. Chem. 14*, 195−202.

Engelborghs, Y., Dumortier, C., D'Hoore, A., Vandecandelaere, A., & Fitzgerald, T. J. (1993) *J. Biol. Chem. 268*, 107−112.

Farrell, K. W., Jordan, M. A., Miller, H. P., & Wilson, L. (1987) *J. Cell Biol. 104*, 1035−1046.

Fishback, J. L., & Yarbrough, L. R. (1984) *J. Biol. Chem. 259*, 1968−1973.

Gildersleeve, R. F., Cross, A. R., Cullen, K. E., Fagen, A. P., & Williams, R. C. (1992) *J. Biol. Chem. 267*, 7995−8006.

Horio, T., & Hotani, H. (1986) *Nature 321*, 605−607.

Hotani, H., & Horio, T. (1988) *Cell Motil. Cytoskeleton 10*, 229−236.

Howard, W. D., & Timasheff, S. N. (1986) *Biochemistry 25*, 8292−8300.

Hyams, J. S., & Lloyd, C., Eds. (1994) *Microtubules*, Wiley-Liss, New York.

Hyman, A. A., Salser, S., Drechsel, D. N., Unwin, N., & Mitchison, T. J. (1992) *Mol. Biol. Cell 3*, 1155−1167.

Jacobs, M., Smith, H., & Taylor, E. W. (1974) *J. Mol. Biol. 89*, 455−468.

Jameson, L., & Caplow, M. (1980) *J. Biol. Chem. 255*, 2284−2292.

Karr, T. L., Prodsky, A. E., & Purich, D. L. (1979) *Proc. Natl. Acad. Sci. U.S.A. 76*, 5475−5479.

Keates, R. A. B., & Mason, G. B. (1981) *Can. J. Biochem. 59*, 361−370.

Koshland, D. E., Mitchison, T. J., & Kirschner, M. W. (1988) *Nature 331*, 499−504.

Kowalski, R. J., & Williams, R. C. (1993a) *J. Biol. Chem. 268*, 9847−9855.

Kowalski, R. J., & Williams, R. C. (1993b) *Cell Motil. Cytoskeleton 26*, 282−290.

Kristofferson, D., Lee, S.-H., Terry, B. J., Saucier, A. C., Karr, T. L., & Purich, D. L. (1982) in *Biological Functions of Microtubules and Related Structures* (Sakai, H., Mohri, H., & Borisy, G. G., Eds.) pp 49−60, Academic Press, London.

Kristofferson, D., Mitchison, T., & Kirschner, M. W. (1986) *J. Cell Biol. 102*, 1007−1019.

MacNeal, R. K., & Purich, D. L. (1978) *J. Biol. Chem. 253*, 4683−4687.

Mandelkow, E.-M., Lange, G., Jagla, A., Spann, U., & Mandelkow, E. (1988) *EMBO J. 7*, 357−365.

Martin, S. R, & Bayley, P. M. (1987) *Biophys. Chem. 27*, 67−76.

Martin, S. R., Schilstra, M. J., & Bayley, P. M. (1987) *Biochem. Biophys. Res. Commun. 149*, 461−467.

Martin, S. R., Schilstra, M. J., & Bayley, P. M. (1993) *Biophys. J. 65*, 578−596.

Mejillano, M. R., Barton, J. S., Nath, J. P., & Himes, R. H. (1990) *Biochemistry 29*, 1208−1216.

Mejillano, M. R., & Himes, R. H. (1991) *Arch. Biochem. Biophys. 291*, 356−362.

Melki, R., Carlier, M.-F., Pantaloni, D., & Timasheff, S. N. (1989) *Biochemistry 28*, 9143−9152.
Melki, R., Carlier, M.-F., & Pantaloni, D. (1990) *Biochemistry 29*, 8921−8932.
Mitchison, T., & Kirschner, M. (1984a) *Nature 312*, 232−237.
Mitchison, T., & Kirschner, M. (1984b) *Nature 312*, 237−242.
O'Brien, E. T., Voter, W. A., & Erickson, H. P. (1987) *Biochemistry 26*, 4148−4156.
O'Brien, E. T., Salmon, E. D., Walker, R. A., & Erickson, H. P. (1990) *Biochemistry 29*, 6648−6656.
Oosawa, F., & Asakura, S. (1975) *Thermodynamics of the Polymerization of Protein*, Academic Press, London.
Pantaloni, D., & Carlier, M.-F. (1986) *Ann. N.Y. Acad. Sci. 466*, 496−509.
Pryer, N. K., Walker, R. A., Skeen, V. P., Bourns, B. D., Sobeiro, M. F., & Salmon, E. D. (1992) *J. Cell Sci. 103*, 965−976.
Roberts, K., & Hyams, J. S. (1979) *Microtubules*, Academic Press, London.
Schilstra, M. J., Martin, S. R., & Bayley, P. M. (1987) *Biochem. Biophys. Res. Commun. 147*, 588−595.
Schilstra, M. J., Martin, S. R., & Bayley, P. M. (1989) *J. Biol. Chem. 264*, 8827−8834.
Schilstra, M. J., Bayley, P. M., & Martin, S. R. (1991) *Biochem. J. 277*, 839−847.
Seckler, R., Wu, G.-M., & Timasheff, S. N. (1990) *J. Biol. Chem. 256*, 7655−7661.
Shearwin, K. E., & Timasheff, S. N. (1992) *Biochemistry 31*, 8080−8089.
Shearwin, K. E., Perez-Ramirez, B., & Timasheff, S. N. (1994) *Biochemistry 33*, 885−893.
Simon, J. R., Parsons, S. F., & Salmon, E. D. (1992) *Cell Motil. Cytoskeleton 21*, 1−14.
Song, Y.-H., & Mandelkow, E. (1993) *Proc. Natl. Acad. Sci. U.S.A. 90*, 1671−1675.
Sternlicht, H., & Ringel, I. (1979) *J. Biol. Chem. 254*, 10540−10550.
Stewart, R. J., Farrell, K. W., & Wilson, L. (1990) *Biochemistry 29*, 6489−6498.
Terry, B. J., & Purich, D. L. (1980) *J. Biol. Chem. 255*, 10532−10536.
Vandecandelaere, A., Martin, S. R., Bayley, P. M., & Schilstra, M. J. (1994) *Biochemistry 33*, 2792−2801.
Walker, R. A., O'Brien, E. T., Pryer, N. K., Sobeiro, M., Voter, W. A., Erickson, H. P., & Salmon, E. D. (1988) *J. Cell. Biol. 107*, 1437−1448.
Walker, R. A., Pryer, N. K., & Salmon, E. D. (1991) *J. Cell Biol. 114*, 73−81.
Weisenberg, R. C., Borisy, G. G., & Taylor, E. W. (1968) *Biochemistry 7*, 4466−4478.
Weisenberg, R. C., Deery, W. J., & Dickinson, P. J. (1976) *Biochemistry 15*, 4248−4254.
Zackroff, R. V., Weisenberg, R. C., & Deery, W. J. (1980) *J. Mol. Biol. 139*, 641−677.
Zeeberg, B., & Caplow, M. (1979) *Biochemistry 18*, 3880−3886.

BI941560B